Iris Recognition for Biometric Identification using Dyadic Wavelet Transform Zero-Crossing

D. de Martin- Roche*, C. Sanchez-Avila† & R. Sanchez-Reillo‡

* Ericsson España S.A., Dpt. Software Engineering, C/ Ombu, 3, 28045 Madrid, Spain.

*Dpto. de Matematica Aplicada, E.T.S.I. Telecomunicacion, Universidad Politecnica de Madrid, 28040 Madrid, Spain.

† Dpto. de Ingenieria Electrica, Electronica y Automatica, Universidad Carlos III de Madrid, 28911 Madrid, Spain.

Abstract - In this work, a new biometric identification approach based on the human iris pattern is proposed. The main idea of this technique is to represent the features of the iris by fine-to-coarse approximations at different resolution levels based on the discrete dyadic wavelet transform zero-crossing representation. The resulting one-dimensional (1-D) signals are compared with model features using different distances. Before performing the feature extraction, a pre-processing step is to be made by image processing techniques, isolating the iris and enhancing the area of study. The proposed technique is translation, rotation and scale invariant. Results will show a classification success above 98% achieving an Equal Error Rate equal to 0,21% and the possibility of having null False Acceptance Rates with low False Rejection Rates.

Introduction

Nowadays, one of the main threats that IT systems and security environments can have, is the possibility of having intruders in the system. This is normally solved by user authentication schemes based on passwords, secret codes and/or identification cards or tokens. Schemes based only on passwords or secret codes can be cracked by intercepting the presentation of such a password, or even by counterfeiting it (via passwords dictionaries or, in some systems, via brutal force attacks). On the other hand, an intruder can attack systems based on identification card or tokens by robbing, copying or simulating them. If the scheme used in the system is based both on a card and a password (usually called Personal Identification Number - PIN), the intruder should apply more effort to gain entry to the system, and with more advanced technologies, such as smart cards, some vulnerabilities of the system could be avoided (e.g. brutal force attacks are impossible under a well-defined smart card).

As it is well-known, biometrics deals with identification of individuals based on their biological and/or behavioral features. Technologies that exploit biometrics have the potential application of identifying individuals in order to control access to secured areas or materials. Nowadays a lot of biometric techniques are being developed based on different features and algorithms. In fact, there are many biometric techniques that are either widely used or under investigation, including voice, face, iris, fingerprint, ear, retinal scan, signature, etc. [3]. Each technique has its strengths and limitations, not being possible to determine which is the best. No single biometrics is expected to effectively meet the needs of all the applications. Nevertheless, it is known that, from all of these techniques, iris recognition is the most promising for high security environments [2]. The biometric identification problem can be categorized into two fundamentally distinct types of problems with different complexities: recognition (or identification) and verification (or authentication). Recognition refers to the problem of establishing a user's identity. Verification refers to the problem of confirming or denying a user's claimed identity. The possibility that the human iris might be used as a kind of optical fingerprint for personal identification was suggested originally by ophthalmologists. Therefore, the potential of the human iris for such kind of problems comes from the anatomy of the eye. Some properties of the human iris that enhance its suitability for use in automatic identification include: 1) its inherent isolation and protection from the external environment, being an internal organ of the eye, behind the cornea and the aqueous humor; 2) the impossibility of surgically modifying it without high risk of damaging the user's vision; and 3) its physiological response to light, which provides the detection of a dead or plastic iris, avoiding this kind of counterfeit. Also several studies have shown that while the general structure of the iris is genetically determined, the particulars of its minutiae are critically dependent on initial conditions in the embryonic mesoderm from wich it develops. Therefore, there are not ever two irises alike, not even for uniovular (identical) twins [2]. In these respects the uniqueness of every iris parallels the uniqueness of every fingerprint. At the moment, only two prototype iris-recognition systems had been developed by Daugman [2] and Wildes et al.[9]. Nevertheless, this biometric technology presents still many open problems. So, more recently, we can find some works in this issue, as given by Boles et al.[1], using wavelet transform, and by Sanchez-Reillo et al. [7], where Gabor filters are used. Here, we develop a new approach using dyadic wavelet transform zero-crossing. A wavelet function that is the first derivative of a cubic spline will be used to construct the representation.

Image Acquisition and Preprocessing

0-7803-6636-0/01/$10.00 ©2001 IEEE

Image Acquisition and Preprocessing

The biological data is captured using a high resolution photo camera. Future work will use capture devices such as video cameras and infrared light. After the capture and before the feature extraction, two steps are performed: the location of the iris inside the image, and a pre-processing block that will transform the image into a 1-D signal.

First, the image of the eye is converted to grayscale and its histogram is stretched. Then, throughout a griding process, the centre of the iris, as well as the outer boundary, i.e. the border between the iris and the sclera, is detected taking profit of the circular structure of the latter. The detection is performed maximising D in the equations shown in (2.1), where (x_0, y_0) is a point in the grid taken as centre, Δ_r and Δ_θ are the increments of radio and angle, and $I(x, y)$ is the image in gray levels.

$$D = \sum_m \sum_{k=1}^{5} (I_{n,m} - I_{n-k,m}) \tag{2.1}$$

being

$$I_{i,j} = I(x_0 + i\Delta_r \cos(j\Delta_\theta),\ y_0 + i\Delta_r \sin(j\Delta_\theta)) \tag{2.2}$$

Once detected the outer bounds of the iris, everything in the image outside it is suppressed, and this same process is performed in order to find the inner boundary, i.e. the frontier between the iris and the pupil. The points inside this last border are also suppressed, obtaining an image like the one showed in Fig.1.

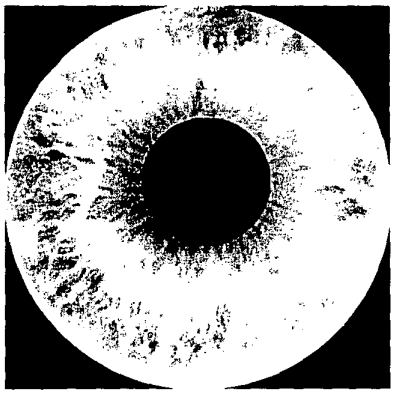

Figure 1: Sample iris image.

In the last step of the pre-processing block, the dimensions of the irises in the images will be scaled to have the same constant diameter regardless of the original size in the images. Then, the centroid of the detected pupil is chosen as the reference point for extracting the features of the iris. Thus, the gray level values on the contours of a virtual circle, which is centered at the centroid of the pupil, are recorded. Such data set (256 bits) will be referred as *iris signature* (IS) (Fig.2).

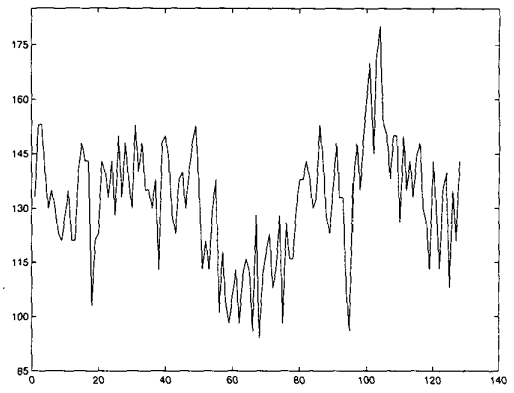

Figure 2: Sample iris signature from the image of Fig.1.

Feature Extraction

In order to use the iris pattern for identification, it is important to define a representation that is well adapted for extracting the iris information content from iris signatures. In this way, we introduce an algorithm for extracting unique features from iris signatures and representing these features using discrete dyadic wavelet transform.

The discrete dyadic wavelet transform

Let $\psi_s(x)$ denote the dilation of a function ψ by a factor (scale) s:

$$\psi_s(x) = \frac{1}{s}\psi\left(\frac{x}{s}\right). \tag{3.1}$$

The continuous wavelet transform of a (continuous) function $f(x)$ at the scale s and position x can be written as the following convolution

$$W_s f(x) = f * \psi_s(x). \tag{3.2}$$

Let us denote by $\hat{\psi}(\omega)$ the Fourier transform of $\psi(x)$. Grossmann and Morlet showed that if $\hat{\psi}(\omega)$ satisfies

$$\int_{-\infty}^{\infty} \frac{|\hat{\psi}(\omega)|^2}{|\omega|}\, d\omega = C_\psi < \infty, \tag{3.3}$$

then $f(x)$ can be reconstructed from its wavelet transform. Condition (3.3) is called the admissibility condition and it implies that

$$\hat{\psi}(0) = 0. \tag{3.4}$$

The term "wavelet" is used for any function from $L^2(\mathbb{R})$ which satisfies the admissibility condition. From (3.4) we see that the wavelet $\psi(x)$ can be interpreted as the impulse response of a band-pass filter. Then, wavelet transform of a function f can be viewed as the response of a family of dilated band-pass filters to a signal f. In practical implementations, both parameters, x and s, of the continuous wavelet transform $W_s f(x)$ have to be discretized. The relationship between continuous and discrete versions of a wavelet transform will be described

carefully. At this point, a discrete set of scales is considered. It turns out, that if

$$\sum_{-\infty}^{\infty} \left|\hat{\psi}\left(2^j\omega\right)\right|^2 = 1, \tag{3.5}$$

then the scale parameter can be sampled along the dyadic sequence $\{2^j\}_{j\in\mathbb{Z}}$ while preserving the reconstruction property. Any wavelet satisfying equation (3.5) is called a dyadic wavelet and the sequence of functions

$$\{W_{2^j} f(x)\}_{j\in\mathbb{Z}} \tag{3.6}$$

is called the dyadic wavelet transform. Nevertheless, in practice, due to finite view or interest, we are limited by a finite largest scale. Due to finite resolution of any measurement equipment, the finest scale is bounded from below as well. For normalization purposes, let us assume that the finest scale is 1 and 2^J is the largest scale. For finite numbers of scales, we need to understand what kind of information is included in

$$\{W_{2^j} f(x)\}_{1\le j\le J}. \tag{3.7}$$

First, let us introduce a scaling function $\phi(x)$ whose Fourier transform, $\hat{\phi}(\omega)$, satisfies

$$\left|\hat{\phi}(\omega)\right|^2 = \sum_{j=1}^{\infty} \left|\hat{\psi}\left(2^j\omega\right)\right|^2. \tag{3.8}$$

Using (3.8) we can prove that

$$\left|\hat{\phi}(\omega)\right|^2 = \sum_{j=1}^{J} \left|\hat{\psi}\left(2^j\omega\right)\right|^2 + \left|\hat{\phi}(2^J\omega)\right|^2, \tag{3.9}$$

and, using (3.5), it can be shown that $\lim_{\omega\to 0}|\hat{\phi}(\omega)| = 1$. Therefore, $\phi(x)$ can be viewed as the impulse response of a low-pass filter or equivalently as a smoothing function. Let us define the smoothing operator S_{2^j} by

$$S_{2^j} f(x) = f \star \phi_{2^j}(x) \tag{3.10}$$

where $\phi_{2^j}(x) = \frac{1}{2^j}\phi\left(\frac{x}{2^j}\right)$. One can derive that the higher frequencies of $S_1 f(x)$, which have disappeared in $S_{2^J} f(x)$, can be recovered from the dyadic wavelet transform $\{W_{2^j} f(x)\}_{1\le j\le J}$. We suppose that the original signal is a discrete sequence f^d of finite energy. If there exists two constants $C_1 > 0$ and $C_2 > 0$ such that $\hat{\phi}(\omega)$ satisfies

$$\forall\omega\in\Omega, \quad C_1 \le \sum_{n=-\infty}^{\infty} \left|\hat{\phi}(\omega + 2n\pi)\right|^2 \le C_2 \tag{3.11}$$

then one can prove that the input signal can be written $f^d = S_1 f[n]$. Let us denote

$$S^d_{2^J} f = (S_{2^J} f[n+w])_{1\le n\le N},\ W^d_{2^j} f = (W_{2^j} f[n+w])_{1\le n\le N}, \tag{3.12}$$

where N is the length of f^d, and w is a sampling shift that depends only on ψ [5]. Then, the discrete dyadic wavelet transform (DDWT) of $f^d = S_1 f[n]$ can be defined as the sequence of discrete signals

$$\left\{\left(W^d_{2^j} f\right)_{1\le j\le J}, S^d_{2^J} f\right\}, \tag{3.13}$$

for any coarse scale 2^J. In this work, a fast discrete wavelet transform algorithm and its inverse has been utilized. A detailed implementation of this algorithm can be found in [4].

Zero-Crossing Representation of Iris Patterns

When a signal includes important structures that belong to different scales, it is often helpful to reorganize the signal information into a set of "detail components" of varying size. It is known that one can obtain the position of multiscale sharp variations points from the zero-crossing of the signal convolved with the laplacian of a gaussian [6]. This procedure has been used in many pattern recognition applications. A fundamental issue is to understand whether the zero-crossing define a complete and stable representation of the original signal. Indeed, for pattern recognition applications, we remove some important components of the signal, when representing it with multiscale zero-crossing.

Let $f \in L^2(\mathbb{R})$ and $\{W_{2^j} f(x)\}_{j\in\mathbb{Z}}$ be its dyadic wavelet transform. For any pair of consecutive zero-crossings of W_{2^j} whose abscissae are respectively (z_{n-1}, z_n), we record the value of the integral

$$e_n = \int_{z_{n-1}}^{z_n} W_{2^j} f\, dx. \tag{3.14}$$

For any function $W_{2^j} f$, the position of the zero-crossings $(z_n)_{n\in\mathbb{Z}}$ can be represented by a piece-wise constant function

$$Z_{2^j} f = \frac{e_n}{z_n - z_{n-1}}, \qquad x \in [z_{n-1}, z_n] \tag{3.15}$$

Therefore, in order to obtaining a complete and stable representation, we consider the zero-crossing of the dyadic wavelet transform of the *iris signature* (IS), i.e. instead of considering the zero-crossing of a wavelet transform on a continuum of scales, we restrict ourselves to dyadic scales 2^j, $j \in Z$, and we also record the value of the wavelet transform between two consecutive zero-crossings.

In practical implementations, the input signal, in our case the iris signature, is measured with a finite resolution that imposes a finer scale when computing the dyadic wavelet transform, and we cannot compute the wavelet transform at all scales 2^j for j varying from $-\infty$ to $+\infty$. We are limited by a finite larger scale and a nonzero finer scale. Let us suppose for normalization purposes that the finer scale is equal to 1 and that 2^J is the largest scale. Therefore, we can obtain the discrete dyadic wavelet transform of the iris signature (IS)

$$\left\{S_{2^J}(IS),\ (W_{2^j}(IS))_{1\le j\le J}\right\} \tag{3.16}$$

where $S_{2^J}(IS)$ is the coarse signal and $(W_{2^j}(IS))_{1\leq j\leq J}$ can be interpreted as the discrete details available when smoothing IS at the scale 1 but which have disappeared when smoothing IS at the larger scale 2^J [7].

Zero crossing of $(W_{2^j}(IS))_{1\leq j\leq J}$ are estimated from sign changes of its samples. The position of each zero-crossing is estimated with a linear interpolation between two samples of different sign. Therefore, if IS has N nonzero samples, since there are at most $N\log(N)$ samples in its discrete wavelet representation, the number of operations to obtain the position of the zero-crossing is $O(Nlog(N))$. Clearly, that from a discrete dyadic wavelet transform, we can only compute the zero-crossing positions along the scales 2^j such that $1 \leq j \leq J$. Therefore, we consider as the discrete zero crossing representation of IS the set of signals

$$\left\{(Z_{2^j}(IS))_{1\leq j\leq J}\right\} \tag{3.17}$$

We have excluded the coarsest level in order to obtain a robust representation in a noisy environment and reduces the number of computations required, since information at fine resolution levels is strongly affected by noise and quantization errors which are due to the use of a rectangular grid in digital images [8]. Thus, to reduce such effects on the zero-crossing representation a few low resolution levels, excluding the coarsest one, will be used. The dyadic wavelet used in this work is the quadratic spline of compact support defined in [5]. The advantage of using this function is that it has a finite support and it also has a smaller number of coefficients than those of the second derivative of a smoothing function [6].

Finally, in order to obtain a robust representation in noisy environments, and to reduce the amount of computations required, only a reduced number of resolutions levels are used. In this work, the four lowest resolution levels, excluding the coarsest, have been used, i.e. $3 \leq j \leq 6$ (Fig. 3).

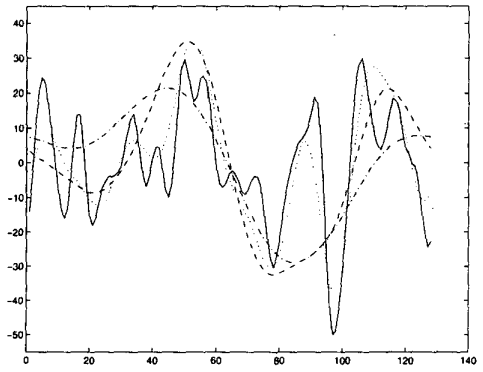

Figure 3: Lowest four resolution levels of the wavelet transform of iris signature (Fig.2).

Fig.4 shows the zero-crossing representation corresponding to the lowest four resolution levels of the wavelet transform previously calculated.

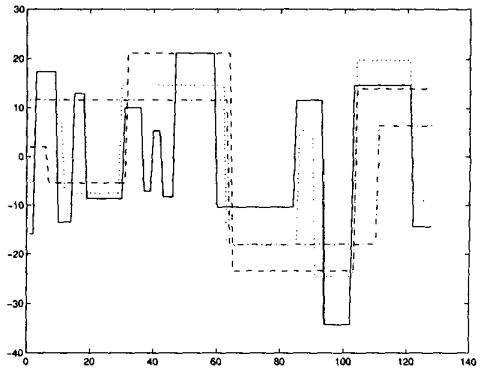

Figure 4: Zero-crossing representation of the iris of Fig.1.

Classification and Verification

All the features obtained should enter a comparison process to determine the user whose iris photograph was taken. This comparison is to be made with the user's template, which will be calculated depending on the comparison algorithm used. The following different methods have been used:

- The euclidean distance, considered the most common technique of all, performs its measurements with the following equation

$$d_E(y,p) = \sqrt{\sum_{i=1}^{L}(y_i - p_i)^2}, \tag{4.1}$$

being L the dimension of the feature vector, y_i the ith component of the sample feature vector, and p_i the ith component of the template feature vector.

- The (binary) Hamming distance

$$d_H^b(y,p) = \frac{1}{L}\sum_{i=1}^{L} y_i \oplus p_i, \tag{4.2}$$

doesn't measure the difference between the components of the feature vectors, but the number of components that differ in value. As it is typical that all the components differ among samples of the same user, it is necessary to follow another approach for template computation different from the one used for the euclidean distance. Based on the assumption that the feature components follow a Gaussian distribution, not only the mean of the set of initial samples is obtained, but also a factor of standard deviation of the samples. In the comparison process, the number of components of the feature vector falling outside the area defined by the template parameters is counted, obtaining the Hamming distance

$$d_H(y,p) = \#\left\{i \in \{1,...,L\} \ : \ |y_i - p_i^m| > p_i^v\right\}, \tag{4.3}$$

where y_i the ith component of the sample vector, p_i^m is the mean for the ith component, and p_i^v the factor of the standard deviation for the ith component.

- Finally, we describe a distance directly related with the zero-crossing representation of a 1-D signal [8]. Let us denote the zero-crossing representation of an object p at a particular resolution level j by $Z_j p$. Also,, let $X_j = \{x_j(r);\ r = 1, ..., R_j\}$, be a set containing the locations of zero-crossing points at level j, where R_j is the number of zero-crossings of he representation at this level. Then, the representation $Z_j p$ can be uniquely expressed in the form of a set of ordered complex numbers whose imaginary, $[\rho_j]_p$, and real, $[\mu_j]_p$, parts indicate the zero-crossing position and magnitude of $Z_j p$ between two adjacent zero-crossing points, respectively. Thus, we consider the following dissimilarity function which compare the unknown object y and candidate model p at a particular resolution level j:

$$d_j(y,p) = \frac{\sum_{i=1}^{R_j} \left\{ [\mu_j(r)]_y [\rho_j(r)]_y - \Gamma [\mu_j(r)]_p [\rho_j(r)]_p \right\}^2}{\Gamma \sum_{i=1}^{R_j} \left| [\mu_j(r)]_y [\rho_j(r)]_y \right| \left| [\mu_j(r)]_p [\rho_j(r)]_p \right|} \tag{4.4}$$

where Γ is the scale factor and equals the ratio between the average radius of the candidate model and that of the unknown object. Note that this function is computed using only the zero-crossing points.

The overall dissimilarity value of the unknown object and the candidate model over the resolution interval $[K, M]$ will be the average of the dissimilarity functions calculated at each resolution level in this interval, i.e.,

$$D_Z(y,p) = \sum_{j=K}^{M} \frac{d_j(y,p)}{K - M - 1}. \tag{4.5}$$

Experimental Results

This section reports some experimental results obtained, detailing the database used, the enrollment process, and final results in classification, i.e. in a biometric recognition scheme, and in biometric verification.

Database

The results have been obtained using a database of both eyes of 10 peoples and, at least, 10 photos of each eye. The photographs were taken in different hours and days, during 7 months. Each eye was considered as "of a different person", i.e. each person has two identities, the one of the left eye, and the one of the right one. That makes 20"virtual" different users.

Results in Recognition

An analysis has been made to obtain results in biometric recognition (i.e., biometric classification), obtaining the results in Table 1. It can be seen that (binary) Hamming distance, applied at each scale of the zero-crossing representation of iris signature, shows the best results, achieving a 97,9 percent of classification success, while the D_Z an Euclidean distances achieve a 95,7 and 93,6 percent of success, respectively.

Distance	Classification Success
Euclidean	93,6 %
Hamming	97,9 %
D_Z	95,7 %

Table 1: Results in classification.

Results in Verification

In a verification system, the performance can be measured in terms of three different rates:

- False Acceptance Rate (FAR): the probability of identifying an intruder as an enrolled user.
- False Rejection Rate (FRR): the probability of rejecting an enrolled user, as if he were an intruder.
- Equal Error Rate (EER): the value where the FAR and FRR rates are equal.

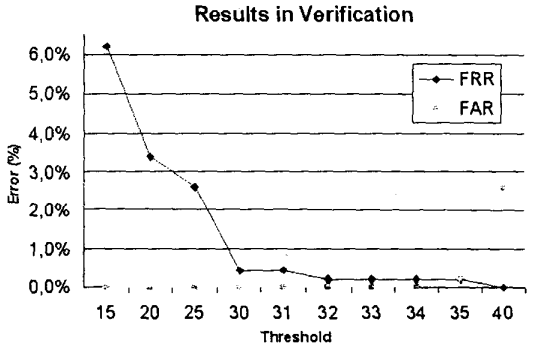

Figure 5: Results in Verification with binary Hamming distance.

In our case, the (binary) Hamming distance still shows the better results. It can be seen in Fig.6, that Equal Error Rate (EER), i.e. the cross point between the FAR and the FRR curves, achieve a 0,21%. But what is more important, is that a null FAR has been obtained for very low rates of False Rejection, which means that this system is optimal for very high security environments.

Conclusions

A biometric identification system, based on the processing of the human iris by the Dyadic Wavelet Transform, has been introduced. The procedure to obtain an *iris signature* of 256 bits has been described, as well as

the feature extraction block and the verification system. The results have shown that the system can achieve high rates of security.

References

[1] W. W. Boles, and B. Boashash, A Human Identification Technique Using Images of the Iris and Wavelet Transform, *IEEE Transactions on Signal Processing*, vol. 46, no 4, pp. 1185-1188, April 1998.

[2] J. Daugman, High confidence visual recognition by test of statistical independence, *IEEE Transactions on Pattern Analysis and Machine Intelligence*, vol. 15, pp. 1148-1161, November 1993.

[3] A. K. Jain, R. Bolle, S. Pankanti S., et al., *Biometrics: Personal Identificacion in Networked Society*, Kluwer Academic Publishers, 1999.

[4] S. Mallat, *A Wavelet Tour of Signal Processing*, Academic Press, 1999.

[5] S. Mallat and S. Zhong, Characterization of Signals from Multiscale Edges, *IEEE Transactions on Pattern Analysis and Machine Intelligence*, vol. 14, no. 7, pp. 710-732, July 1992.

[6] S. Mallat, Zero-Crossings of a Wavelet Transform, *IEEE Transactions on Information Theory*, vol 37, no. 4, pp 1019-1033, July 1991.

[7] R. Sanchez-Reillo and C. Sanchez-Avila, Processing of the Human Iris Pattern for Biometric Identification *Proc. of IPMU 2000 (8^{th} International Conference on Information Processing and Management of Uncertainty in Knowledge Based Systems)* (Madrid, Spain), pp. 653-656, 3-7 July, 2000.

[8] Q. M. Tieng, and W. W. Boles, Recognition of 2D Object Contours Using the Wavelet Transform Zero-Crossing Representation, *IEEE transactions on Pattern Analysis and Machine Intelligence*, vol. 19, no. 8, pp 910-916, August 1997.

[9] R. Wildes et al., A system for automated iris recognition, *Proc. 2nd IEEE Workshop Applicat. Comput. Vision*, pp. 121-128, December 1994.